

# 48

## Low-Power Laser Therapy

48.1	Introduction .....	48-1
48.2	Clinical Applications and Effects of Light Coherence and Polarization .....	48-2
	Coherence of Light • Coherence of Light Interaction with Biomolecules, Cells, and Tissues	
48.3	Enhancement of Cellular Metabolism via Activation of Respiratory Chain: A Universal Photobiological Action Mechanism .....	48-7
	Cytochrome <i>c</i> Oxidase as the Photoacceptor in the Visible-to- Near-Infrared Spectral Range • Primary Reactions after Light Absorption • Cellular Signaling (Secondary Reactions) • Partial Derepression of Genome of Human Peripheral Lymphocytes: Biological Limitations of Low-Power Laser Effects	
48.4	Enhancement of Cellular Metabolism via Activation of Nonmitochondrial Photoacceptors: Indirect Activation/Suppression .....	48-18
48.5	Conclusion .....	48-20
	Acknowledgments .....	48-20
	References .....	48-20

**Tiina I. Karu**

*Institute of Laser and  
Information Technologies  
Russian Academy of Sciences  
Troitsk, Moscow Region,  
Russian Federation*

### 48.1 Introduction

The first publications about low-power laser therapy (then called laser biostimulation) appeared more than 30 years ago. Since then, approximately 2000 studies have been published on this still controversial topic.<sup>1</sup> In the 1960s and 1970s, doctors in Eastern Europe, and especially in the Soviet Union and Hungary, actively developed laser biostimulation. However, scientists around the world harbored an open skepticism about the credibility of studies stating that low-intensity visible-laser radiation acts directly on an organism at the molecular level. The coherence of laser radiation for achieving stimulative effects on biological objects was more than suspect. Supporters in Western countries, such as Italy, France, and Spain, as well as in Japan and China also adopted and developed this method, but the method was — and still remains — outside mainstream medicine. The controversial points of laser biostimulation,<sup>2-4</sup> which were topics of great interest at that time, were analyzed in reviews that appeared in the late 1980s.

Since then, medical treatment with coherent-light sources (lasers) or noncoherent light (light-emitting diodes, LEDs) has passed through its childhood and adolescence. Most of the controversial points from “childhood” are no longer topical. Currently, low-power laser therapy — or low-level laser therapy (LLLT) or photobiomodulation — is considered part of light therapy as well as part of physiotherapy. In fact, light therapy is one of the oldest therapeutic methods used by humans (historically as sun therapy, later as color light therapy and UV therapy). A short history of experimental work with colored light on

various kinds of biological subjects can be found elsewhere.<sup>2,3</sup> The use of lasers and LEDs as light sources was the next step in the technological development of light therapy.

It is clear now that laser therapy cannot be considered separately from physiotherapeutic methods that use such physical factors as low-frequency pulsed electromagnetic fields; microwaves; time-varying, static, and combined magnetic fields; focused ultrasound; direct-current electricity; etc. Some common features of biological responses to physical factors have been briefly analyzed.<sup>5</sup>

As this handbook makes abundantly clear, by the dawn of the 21st century, a certain level of development of (laser) light use in therapy and diagnostics (e.g., photodynamic therapy, optical tomography, etc.) had been achieved. In low-power laser therapy, the question is no longer whether light has biological effects but rather how radiation from therapeutic lasers and LEDs works at the cellular and organism levels and what the optimal light parameters are for different uses of these light sources.

This chapter is organized as follows. First, Section 48.2 briefly reviews clinical applications and considers one of the most topical issues in low-power-laser medicine today, i.e., whether coherent and polarized light has additional benefits in comparison with noncoherent light at the same wavelength and intensity.

Second, direct activation of various types of cells via light absorption in mitochondria is described. Primary photoacceptors and mechanisms of light action on cells as well as mechanisms of cellular signaling are considered (Section 48.3). Section 48.4 describes enhancement of cellular metabolism via activation of nonmitochondrial photoacceptors and possible indirect effects via secondary cellular messengers, which are produced by cells as a result of direct activation. This chapter does not consider systemic effects of low-power laser therapy.

## 48.2 Clinical Applications and Effects of Light Coherence and Polarization

Low-power laser therapy is used by physiotherapists (to treat a wide variety of acute and chronic musculoskeletal aches and pains), by dentists (to treat inflamed oral tissues and to heal diverse ulcerations), by dermatologists (to treat edema, indolent ulcers, burns, and dermatitis), by rheumatologists (to relieve pain and treat chronic inflammations and autoimmune diseases), and by other specialists, as well as general practitioners. Laser therapy is also widely used in veterinary medicine (especially in racehorse-training centers) and in sports-medicine and rehabilitation clinics (to reduce swelling and hematoma, relieve pain, improve mobility, and treat acute soft-tissue injuries). Lasers and LEDs are applied directly to the respective areas (e.g., wounds, sites of injuries) or to various points on the body (acupuncture points, muscle-trigger points). Several books provide details of clinical applications and techniques used.<sup>1,6,7</sup>

Clinical applications of low-power laser therapy are diverse. The field is characterized by a variety of methodologies and uses of various light sources (lasers, LEDs) with different parameters (wavelength, output power, continuous-wave or pulsed operation modes, pulse parameters). Figure 48.1 presents schematically the types of light therapeutic devices, possible wavelengths they can emit, and maximal output power used in therapy. The GaAlAs diodes are used in both diode lasers and LEDs; the difference is whether the device contains the resonator (as the laser does) or not (LED). In recent years, longer wavelengths (~800 to 900 nm) and higher output powers (to 100 mW) have been preferred in therapeutic devices.

One of the most topical and widely discussed issues in the low-power-laser-therapy clinical community is whether the coherence and polarization of laser radiation have additional benefits as compared with monochromatic light from a conventional light source or LED with the same wavelength and intensity.

Two aspects of this problem must be distinguished: the *coherence of light* itself and the *coherence of the interaction* of light with matter (biomolecules, tissues).

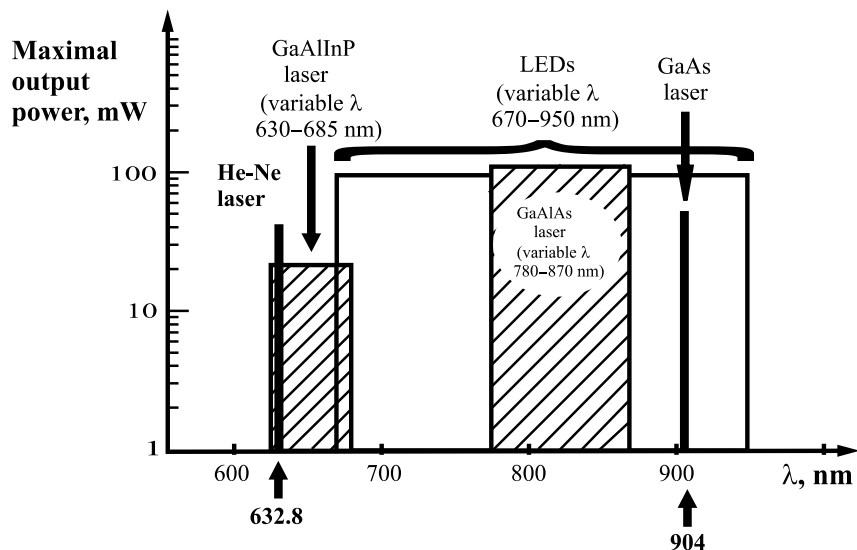


FIGURE 48.1 Wavelength and maximal output power of lasers and LEDs used in low-power laser therapy.

### 48.2.1 Coherence of Light

The coherent properties of light are described by *temporal* and *spatial* coherence. Temporal coherence of light is determined by the spectral width,  $\Delta\nu$ , since the coherence time  $\tau_{\text{coh}}$  during which light oscillates at the point of irradiation has a regular and strongly periodical character:

$$\tau_{\text{coh}} \cong \frac{1}{\Delta\nu} \quad (48.1)$$

Here  $\Delta\nu$  is the spectral width of the beam in Hz. Since light propagates at the rate  $c = 3 \times 10^{10}$  cm/sec, the light oscillations are matched by the phase (i.e., they are coherent) on the length of light propagation  $L_{\text{coh}}$ .

$$L_{\text{coh}} = \frac{c}{\Delta\nu [\text{Hz}]} \quad (48.2)$$

or

$$L_{\text{coh}} = \frac{1}{\Delta\nu [\text{cm}^{-1}]} \quad (48.2)$$

$L_{\text{coh}}$  is called longitudinal coherence. The more monochromatic the light, the longer the length where the light field is coherent in volume. For example, for a multimode He-Ne laser with  $\Delta\nu = 500$  MHz,  $L_{\text{coh}} = 60$  cm. But for a LED emitting at  $\lambda = 800$  nm ( $= 12,500 \text{ cm}^{-1}$ ),  $\Delta\nu = 160 \text{ cm}^{-1}$  (or  $\Delta\lambda = 10$  nm), and  $L_{\text{coh}} = 1/160 \text{ cm}^{-1} \cong 60 \text{ } \mu\text{m}$ , i.e.,  $L_{\text{coh}}$  is longer than the thickness of a cell monolayer ( $\approx 10$  to  $30 \text{ } \mu\text{m}$ ).

Spatial coherence describes the correlation between the phases of the light field in a lateral direction. For this reason, spatial coherence is also called lateral coherence. The size of the lateral coherence ( $\ell_{\text{coh}}$ ) is connected with the divergence ( $\phi$ ) of the light beam at the point of irradiation:

$$\ell_{\text{coh}} \cong \frac{\lambda}{\phi} \quad (48.3)$$

For example, for a He-Ne laser, which operates in the TEM<sub>00</sub> mode, the divergence of the beam is determined by the diffraction:

$$\varphi \equiv \frac{\lambda}{D} \quad (48.4)$$

where  $D$  is the beam diameter. In this case,  $\ell_{\text{coh}}$  coincides with the beam diameter, since for the TEM<sub>00</sub> laser mode the phase of the field along the wave front is constant.

With conventional light sources, the size of the emitting area is significantly larger than the light wavelength, and various parts of this area emit light independently or noncoherently. In this case, the size of the lateral coherence  $\ell_{\text{coh}}$  is significantly less than the diameter of the light beam, and  $\ell_{\text{coh}}$  is determined by the light divergence, as shown in Equation 48.3.

An analysis of published clinical results from the point of view of various types of radiation sources does not lead to the conclusion that lasers have a higher therapeutic potential than LEDs. But in certain clinical cases the therapeutic effect of coherent light is believed to be higher.<sup>1</sup> However, when human peptic ulcers were irradiated by a He-Ne laser or properly filtered red light was irradiated in a specially designed clinical double-blind study, equally positive results were documented for both types of radiation sources<sup>8</sup> (for a review, see Reference 3).

### 48.2.2 Coherence of Light Interaction with Biomolecules, Cells, and Tissues

The coherent properties of light are not manifested when the beam interacts with a biotissue on the molecular level. This problem was first considered several years ago.<sup>2</sup> The question then arose of whether coherent light was needed for “laser biostimulation” or was it simply a photobiological phenomenon. The conclusion was that under physiological conditions the absorption of low-intensity light by biological systems is of purely noncoherent (i.e., photobiological) nature because the rate of decoherence of excitation is many orders of magnitude higher than the rate of photoexcitation. The time of decoherence of photoexcitation determines the interaction with surrounding molecules (under normal conditions less than 10<sup>-12</sup> sec). The average excitation time depends on the light intensity (at an intensity of 1 mW/cm<sup>2</sup> this time is around 1 sec). At 300 K in condensed matter for compounds absorbing monochromatic visible light, the light intensity at which the interactions between coherent light and matter start to occur was estimated to be above the GW/cm<sup>2</sup> level.<sup>2</sup> Note that the light intensities used in clinical practice are not higher than tens or hundreds of mW/cm<sup>2</sup>. Indeed, the stimulative action of various bands of visible light at the level of organisms and cells was known long before the advent of the laser. Also, specially designed experiments at the cellular level have provided evidence that coherent and noncoherent light with the same wavelength, intensity, and irradiation time provide the same biological effect.<sup>9-11</sup> Successful use of LEDs in many areas of clinical practice also confirms this conclusion.

Therefore, it is possible that the effects of light coherence are manifested at the macroscopic (e.g., tissue) level at various depths ( $L$ ) of irradiated matter. Figure 48.2 presents the coherence volumes ( $V_{\text{coh}}$ ) and coherence lengths ( $L_{\text{coh}}$ ) for four different light sources. Figure 48.2A presents the data for two coherent-light sources (He-Ne and diode lasers as typical examples of therapeutic devices). Figure 48.2B presents the respective data for noncoherent light (LED and spectrally filtered light from a lamp). Figure 48.2 illustrates how large volumes of tissue are irradiated only by laser sources with monochromatic radiation (Figure 48.2A). For noncoherent-radiation sources (Figure 48.2B) the length of the coherence,  $L_{\text{coh}}$ , is small. This means that only surface layers of an irradiated substance can be achieved by coherent light.

The spatial (lateral) coherence of the light source is unimportant due to strong scattering of light in biotissue when propagated to the depth  $L \gg l_{\text{sc}}$ , where  $l_{\text{sc}}$  is the free pathway of light in relation to scattering. This is because every region in a scattering medium is illuminated by radiation with a wide angle ( $\varphi \approx 1$  rd). This means that  $\ell_{\text{coh}} \equiv \lambda$ , i.e., the size of spatial coherence  $\ell_{\text{coh}}$ , decreases to the light wavelength (Figure 48.2).

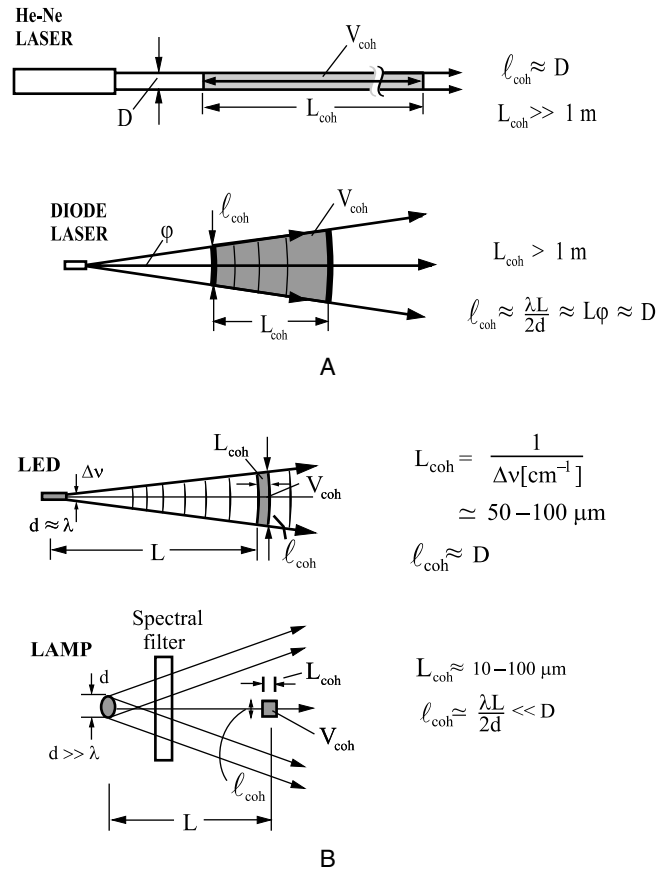


**FIGURE 48.2** Coherence volumes and coherence lengths of light from: (A) laser and (B) conventional sources when a tissue is irradiated.  $L_{\text{coh}}$  = length of temporal (longitudinal) coherence,  $l_{\text{coh}}$  = size of spatial (lateral) coherence,  $D$  = diameter of light beam,  $d$  = diameter of noncoherent-light source,  $\phi$  = beam divergence,  $\Delta\nu$  = beam spectral width.

Thus, the length of longitudinal coherence ( $L_{\text{coh}}$ ) is important when bulk tissue is irradiated because this parameter determines the volume of the irradiated tissue,  $V_{\text{coh}}$ . In this volume, the random interference of scattered light waves and formation of random nonhomogeneities of intensity in space (speckles) occur. For noncoherent-light sources, the coherence length is small (tens to hundreds of microns). For laser sources, this parameter is much higher. Thus, the additional therapeutic effect of coherent radiation, if this indeed exists, depends not only on the length of  $L_{\text{coh}}$  but also, and even mainly, on the penetration depth into the tissue due to absorption and scattering, i.e., by the depth of attenuation. Table 48.1 summarizes qualitative characteristics of coherence of various light sources, as discussed above.

The difference in the coherence length  $L_{\text{coh}}$  is unimportant when thin layers are irradiated inasmuch as the longitudinal size of irradiated object  $\Delta\ell$  is less than  $L_{\text{coh}}$  for any source of monochromatic light (filtered lamp light, LED, laser). Examples are the monolayer of cells and optically thin layers of cell suspensions (Figure 48.3A and B). Indeed, experimental results<sup>9-11</sup> on these models provide clear evidence that the biological responses of coherent and noncoherent light with the same parameters are equal. The situation is quite different when a bulk tissue is irradiated (Figure 48.3C). The coherence length  $L_{\text{coh}}$  is very short for noncoherent-light sources and can play some role only on surface layers of the tissue with thickness  $\Delta\ell_{\text{surface}}$ . For coherent-light sources, the coherence of the radiation is retained along the entire penetration depth  $L$ . The random interference of light waves of various directions occurs over this entire distance in bulk tissue ( $\Delta\ell_{\text{bulk}}$ ). As a result, a speckle pattern of intensity appears. Maximum values of

**TABLE 48.1** Comparison of Coherence (Temporal and Spatial) of Various Light Sources Used in Clinical Practice and Experimental Work

Light Source	Qualitative Characteristics of Coherence			
	Temporal Coherence	Length of Longitudinal (Temporal) Coherence, $L_{coh}$	Spatial Coherence	Volume of Spatial (Lateral) Coherence, $\ell_{coh}$
Laser	Very high	Very long	Very high	Large
LED	Low	Short ( $\gg \lambda$ )	High	Small (very thin layer)
Lamp with a spectral filter	Low	Short ( $\gg \lambda$ )	Very low	Very small
Lamp	Very low	Very short ( $\approx \lambda$ )	Very low ( $\approx \lambda$ )	Extremely small ( $\approx \lambda^3$ )

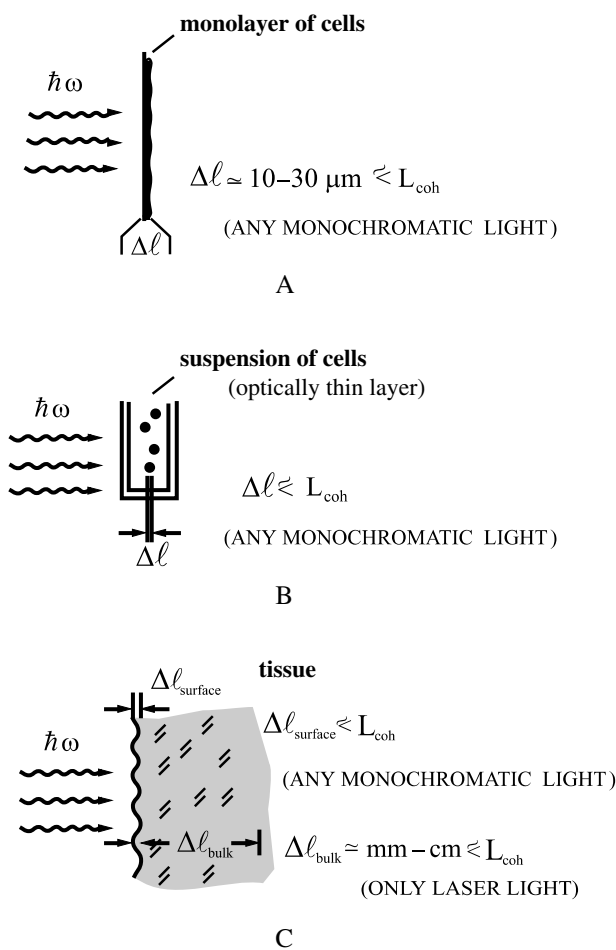


**FIGURE 48.3** Depth ( $\Delta \ell$ ) in which the beam coherency is manifested and coherence length  $L_{coh}$  in various irradiated systems: (A) monolayer of cells, (B) optically thin suspension of cells, and (C) surface layer of tissue and bulk tissue.

the intensity appear at the random constructive interference. The minima (i.e., regions of zero intensity) occur at the random destructive interference. The dimensions of these speckles at every occurrence of directed random interference are approximately within the range of the light wavelength,  $\lambda$ . The coherent effects (speckles) appear only at the depth  $L_{coh}$ . These laser-specific speckles cause a spatially nonhomogeneous

deposition of light energy and lead to statistically nonhomogeneous photochemical processes, an increase in temperature, changes in local pressure, deformation of cellular membranes, etc.

For nonpolarized coherent light the random speckles are less pronounced (they have lower contrast) as compared to the speckles caused by coherent polarized light. A special feature of nonpolarized coherent radiation is that the regions with zero intensity appear less often as compared with the action of coherent polarized light. Thus, the polarization of light causes brighter random intensity gradients that can enhance the manifestation of the effects of light coherence when the tissue is irradiated.

Thus, perhaps in scattering biotissue, the main role is played by coherence length (monochromaticity of light) inasmuch as this parameter determines the depth of tissue where the coherent properties of the light beam can potentially be manifested, depending on the attenuation. This is the spatial (lateral) coherence of the beam, i.e., its directivity, which plays the main role in the delivery of light into biotissue. In addition, the direction and orientation of laser radiation could be important factors for some types of tissues (e.g., dental tissue) that have fiber-type structures (filaments). In this case, waveguide propagation effects of light can appear that provide an enhancement of penetration depth.

Considered within the framework of this qualitative picture, some additional (i.e., additional to those effects caused by light absorption by photoacceptor molecules) manifestation of light coherence for deeper tissue is quite possible. This qualitative picture also explains why coherent and noncoherent light with the same parameters produce the same biological effects on cell monolayer,<sup>9</sup> thin layers of cell suspension,<sup>10,11</sup> and tissue surface (e.g., by healing of peptic ulcers<sup>8</sup>). Some additional (therapeutic) effects from the coherent and polarized radiation can appear only in deeper layers of the bulk tissue. To date, no experimental work has been performed to qualitatively and quantitatively study these possible additional effects. In any case, the main therapeutic effects occur due to light absorption by cellular photoacceptors.

## 48.3 Enhancement of Cellular Metabolism via Activation of Respiratory Chain: A Universal Photobiological Action Mechanism

### 48.3.1 Cytochrome *c* Oxidase as the Photoacceptor in the Visible-to-Near-Infrared Spectral Range

Photobiological reactions involve the absorption of a specific wavelength of light by the functioning photoacceptor molecule. The photobiological nature of low-power laser effects<sup>2,3</sup> means that some molecule (photoacceptor) must first absorb the light used for the irradiation. After promotion of electronically excited states, primary molecular processes from these states can lead to a measurable biological effect at the cellular level. The problem is knowing which molecule is the photoacceptor. When considering the cellular effects, this question can be answered by action spectra.

A graph representing photoresponse as a function of wavelength  $\lambda$ , wave number  $\lambda^{-1}$ , frequency  $\nu$ , or photon energy  $e$  is called an action spectrum. The action spectrum of a biological response resembles the absorption spectrum of the photoacceptor molecule. The existence of a structured action spectrum is strong evidence that the phenomenon under study is a photobiological one (i.e., primary photoacceptors and cellular signaling pathways exist).<sup>12,13</sup>

The first action spectra in the visible-light region were recorded in the early 1980s for DNA and RNA synthesis rate,<sup>14,15</sup> growth stimulation of *Escherichia coli*,<sup>10,16</sup> and protein synthesis by yeasts<sup>16</sup> for the purpose of investigating the photobiological mechanisms of laser biostimulation. In addition, other action spectra were recorded in various ranges of visible wavelengths: photostimulation of formation of E-rosettes by human lymphocytes, mitosis in L cells, exertion of DNA factor from lymphocytes in the violet-green range,<sup>17</sup> and oxidative phosphorylation by mitochondria in the violet-blue range.<sup>18</sup> All these

spectra were recorded for narrow ranges of the optical spectrum and with a limited number of wavelengths, which prevented identification of the photoacceptor molecule.

Full action spectra from 313 to 860 nm for DNA and RNA synthesis rate in both exponentially growing and plateau-phase HeLa cells were also recorded in the early 1980s<sup>19,20</sup> (for a review, see References 2 and 4). The question of the nature of the photoacceptor molecule has since remained open. It was suggested in 1988<sup>21</sup> (see also Reference 4) that the mechanism of low-power laser therapy at the cellular level was based on the absorption of monochromatic visible and NIR radiation by components of the cellular respiratory chain. Absorption and promotion of electronically excited states cause changes in redox properties of these molecules and acceleration of electron transfer (primary reactions). Primary reactions in mitochondria of eukaryotic cells were supposed to be followed by a cascade of secondary reactions (photosignal transduction and amplification chain or cellular signaling) occurring in cell cytoplasm, membrane, and nucleus<sup>21</sup> (for a review, see References 4 and 22). In 1995, an analysis of five action spectra suggested that the primary photoacceptor for the red-NIR range in mammalian cell is a mixed-valence form of cytochrome *c* oxidase<sup>23</sup> (for a review, see Reference 22).

It is remarkable that the five action spectra that were analyzed had very close (within the confidence limits) peak positions in spite of the fact that these processes occurred in different parts of the cells (nucleus and plasma membrane).<sup>19,20,24</sup> However, there were differences in peak intensities. Three of these action spectra only for the red-to-NIR range (wavelengths that are important in low-power laser therapy) are presented in Figure 48.4A, B, and C. Two conclusions were drawn from the action spectra. First, the fact that the peak positions are the same suggests that the primary photoacceptor is the same. Second, the existence of the action spectra implies the existence of cellular signaling pathways inside the cell between photoacceptor and the nucleus as well as between the photoacceptor and cell membrane.

Five action spectra were analyzed, and the bands were identified by analogy with the absorption spectra of the metal-ligand system characteristic of this spectral range<sup>23</sup> (for a review, see References 22 and 25). It was concluded that the ranges 400 to 450 nm and 620 to 680 nm were characterized by the bands pertaining to a complex associated with charge transfer in a metal-ligand system, and within 760 to 830 nm these were d-d transitions in metals, most probably in Cu (II). The range 400 to 420 nm was found to be typical of a  $\pi$ - $\pi^*$  transition in a porphyrin ring. A comparative analysis of lines of possible d-d transitions and charge-transfer complexes of Cu with our action spectra suggested that the photoacceptor was the terminal enzyme of the mitochondrial respiratory chain cytochrome *c* oxidase. It was suggested that the main contribution to the 825-nm band was made by the oxidized  $Cu_A$ , to the 760-nm band by the reduced  $Cu_B$ , to the 680-nm band by the oxidized  $Cu_B$ , and to the 620-nm band by the reduced  $Cu_A$ . The 400- to 450-nm band was more likely the envelope of a few absorption bands in the 350- to 500-nm range (i.e., a superposition of several bands). Analysis of the band shapes in the action spectra and the line-intensity ratios also led to the conclusion that cytochrome *c* oxidase cannot be considered a primary photoacceptor when fully oxidized or fully reduced but only when it is in one of the intermediate forms (partially reduced or mixed-valence enzyme)<sup>23</sup> (for a review, see Reference 22) that have not yet been identified.

Taken together, the terminal respiratory-chain oxidases in eukaryotic cells (cytochrome *c* oxidase) and in prokaryotic cells of *E. coli* (cytochrome *bd* complex<sup>26</sup>) are believed to be photoacceptor molecules for red to NIR radiation. In the violet-to-blue spectral range, flavoproteins (e.g., NADH-dehydrogenase<sup>5,21</sup> in the beginning of the respiratory chain) are also among the photoacceptors and terminal oxidases.

One important step in identifying the photoacceptor molecule is to compare the absorption and action spectra. For recording the absorption of a cell monolayer and investigating the changes in absorption under irradiation at various wavelengths of monochromatic light, a sensitive multichannel registration method was developed.<sup>27,28</sup> Figure 48.4D presents an absorption spectrum of a monolayer of HeLa cells dried in air. In these cells, cytochrome *c* oxidase is fully oxidized. A comparison of the peak position of the spectrum in Figure 48.4D and the action spectra in Figure 48.4A, B, and C shows that the peaks near 620, 680, and 820 nm are present in all four spectra, but the peak near 760 nm is practically absent in the absorption spectrum of dry monolayer HeLa cells. Note the suggestion that this peak belongs to  $Cu_B$  in reduced state.<sup>23</sup>



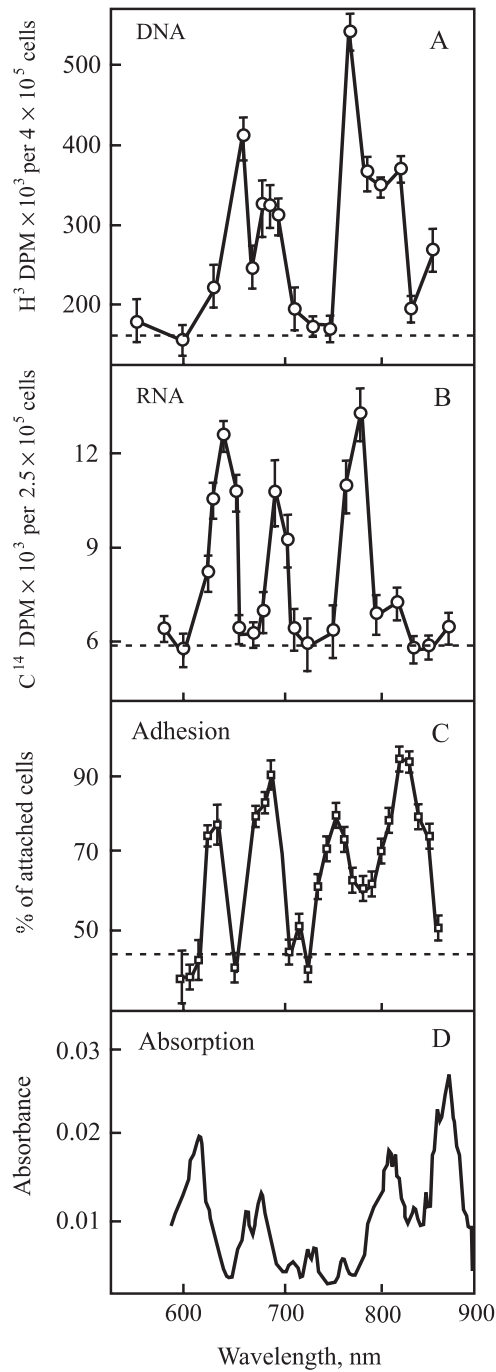


**FIGURE 48.4** Action spectra of (A) DNA and (B) RNA synthesis rate; (C) plasma membrane adhesion of exponentially growing HeLa cells for red to NIR radiation; (D) absorption spectrum of air-dried monolayer of HeLa cells for the same spectral region. (Modified from Karu, T.I. et al., *Nuov. Cim. D*, 3, 309, 1984; Karu, T.I. et al., *Dokl. Akad. Nauk (Moscow)*, 360, 267, 1998; and Karu, T.I. et al., *Lasers Surg. Med.*, 18, 171, 1996.)

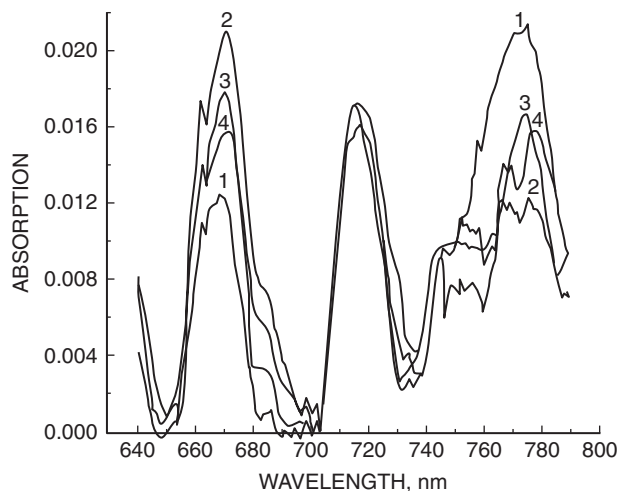


**FIGURE 48.5** Absorption spectrum of monolayer of HeLa cells recorded in open vial immediately after removal of the nutrient medium (curve 1) and following exposure to radiation with  $\lambda = 820$  nm for the first time (curve 2), second time (curve 3), and third time (curve 4), with each exposure lasting 10 sec for a dose  $6.3 \times 10^3$  J/m<sup>2</sup>. (Modified from Karu, T.I. et al., *Dokl. Akad. Nauk (Moscow)*, 360, 267, 1998.)

Later, the absorption spectra were recorded in the monolayer of living HeLa cells, and redox absorbance changes after laser irradiation at different wavelengths were recorded.<sup>27,28</sup> These experiments were performed in open<sup>27</sup> or closed<sup>28</sup> vials. These two conditions differ by, respectively, the partial pressure of oxygen in nutrient medium of cells and by the oxidation state of cytochrome *c* oxidase.

The absorption spectra of a monolayer of living cells in open flasks clearly show the bands at 670 and 775 nm as well as a less distinct band shoulder in the vicinity of 750 nm and band at 718 nm.<sup>27</sup> Exposing the sample for 10 sec to laser radiation with a wavelength of 670 nm and dose of  $6.3 \times 10^3$  J/m<sup>2</sup> caused changes in its absorption bands around 670, 750, and 775 nm, with the absorption band at 718 nm remaining unchanged. In the action spectra, the band in the neighborhood of 670–680 nm supposedly belongs to the chromophore Cu<sub>b</sub> in the oxidized state, while that in the vicinity of 760–770 nm belongs to the chromophore Cu<sub>b</sub> in the reduced state.<sup>23</sup> If there is a correspondence between the action spectra bands (Figure 48.4A, B, and C) and the absorption spectra bands recorded in Reference 27, the results are quite natural: as laser irradiation increases absorption in the band at 670 nm — and hence the concentration of the chromophore in the oxidized state, represented by the absorption near 750–770 nm (and the concentration of the reduced chromophore) — decreases.

The exposure of the cellular monolayer to laser light with  $\lambda = 820$  nm<sup>27</sup> was also observed to cause changes in the absorption bands in the vicinity of 670 and 775 nm (Figure 48.5). Note that the action-spectrum band at around 825 nm is supposedly associated with the oxidized chromophore Cu<sub>A</sub>.<sup>23</sup> Following the first exposure (curve 2), a sharp increase in absorption is observed to occur in the band near 670 nm (and a correspondingly sharp reduction of absorption in the band near 775 nm in comparison with the control, curve 1). The second (curve 3) and the third (curve 4) exposures cause no sharp changes in absorption, which could be due to an equilibrium being established between the oxidized and reduced forms of the chromophore Cu<sub>b</sub>.

In another set of experiments, the HeLa-cell monolayer was irradiated in the closed vial where the cells had been grown for 72 h.<sup>28</sup> Under these conditions, the respiratory chains are supposedly more reduced as compared with the chains in the previous experiments.<sup>27</sup> The spectrum recorded before the irradiation had strong absorption peaks at 739, 757, and 775 nm and weak maxima at 795, 812, 831, and 873 nm, as well as at 630 nm (Figure 48.6A). A comparison of two sets of spectra<sup>27,28</sup> allows for a rough estimation that the peaks in the red (620 to 680 nm) and NIR regions (812 to 870 nm) are characteristic of the absorption spectra of the more oxidized cytochrome *c* oxidase, and the peaks in the 730- to 775-nm

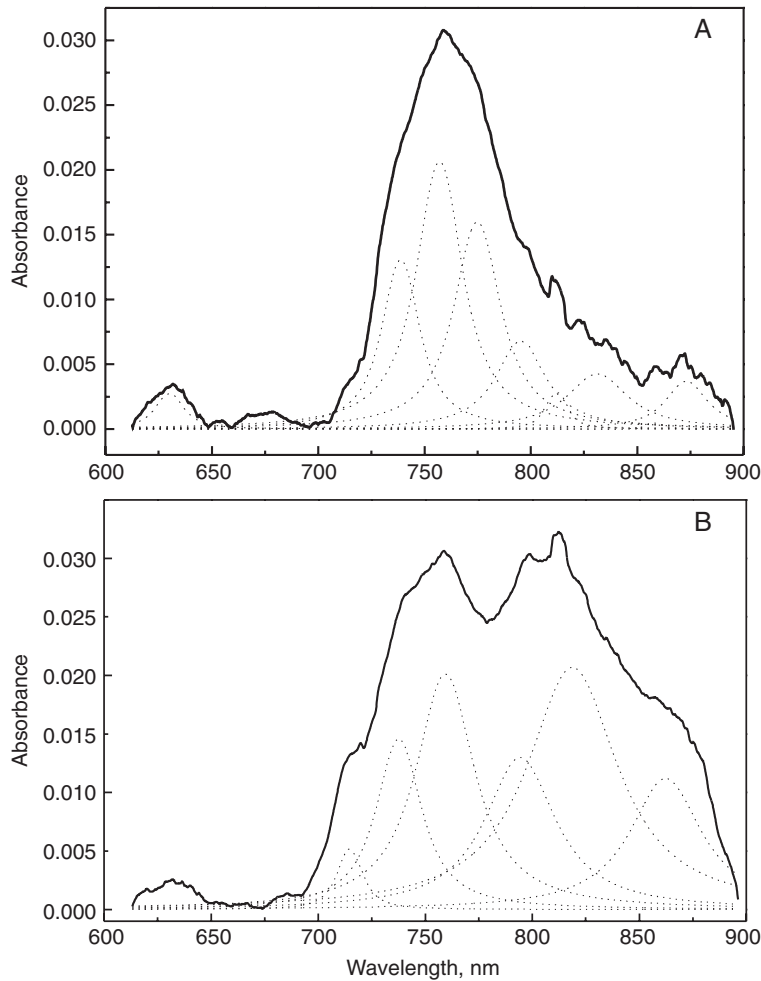




**FIGURE 48.6** Absorption spectra of HeLa monolayer: (A) before and (B) after irradiation at 820, 670, 632.8, and 670 nm in the closed vial (dose at every wavelength  $6.3 \times 10^3$  J/m<sup>2</sup>, irradiation time 10 sec). The dashed lines present the data of Lorentzian fitting of the spectra. (Modified from Karu, T.I. et al., *IEEE J. Sel. Top. Quantum Electron.*, 7, 982, 2001.)



range are characteristic of the spectra of the more reduced cytochrome *c* oxidase. Irradiation of the same HeLa cell monolayer in closed vials at 820, 670, and 632.8 nm and once more at 670 nm caused remarkable changes for the peaks at 739 to 799 nm and at 812 to 873 nm. There were practically no changes in absorption bands in the red region (600 to 700 nm), and a few changes occurred in the green region (peaks at 545 to 581 nm) (Figure 48.6B). It was concluded that cytochrome *c* became more oxidized due to irradiation.<sup>28</sup> The fact that cytochrome *c* oxidase became more oxidized when the tissue or whole cells were irradiated indicates that the oxidative metabolism had been increased.<sup>29</sup> Remarkable redox absorbance changes near 750 to 760 and 820 to 870 nm<sup>28</sup> suggest that irradiation induces structural and functional<sup>30</sup> changes near Cu<sub>A</sub> and Cu<sub>B</sub> chromophores, respectively. The alteration of peak parameters (width, height, area) at 750 to 760 nm indicates that the structure of the *a*<sub>3</sub>-Cu<sub>B</sub> site (probably due to ligand-metal interactions) changes.<sup>29,30</sup> Recall that the irradiation of prokaryotic cells *E. coli* with a He-Ne laser also caused partial oxidation of the terminal part of the respiratory chain, cytochrome *bd* complex, while flavoproteins became slightly reduced.<sup>31</sup>

Changes in the absorption of HeLa cells were accompanied by conformational changes in the molecule of cytochrome *c* oxidase (measured by circular dichroism [CD] spectra<sup>32,33</sup>). In the visible spectral range,



**(1) ACTION SPECTRUM = ABSORPTION SPECTRUM OF MITOCHONDRIA**

550, 565, 575,  
605, 620 nm  myocardium of  
*Helix pomatia*  modifications of  
period and amplitude  
in electrograms<sup>34</sup>

**(2) ACTIVATION IS ACHIEVED WHEN THE MITOCHONDRIAL AREA OF A CELL IS IRRADIATED BY MICROIRRADIATION TECHNIQUE**

488, 514,  
532 nm  rat  
myocardial  
cell  activation in contractibility  
and electrical activity and  
beating frequency<sup>35-38</sup>

**(3) IN EXPERIMENTS PERFORMED BY MICROIRRADIATION TECHNIQUE, INHIBITORS OF RESPIRATORY CHAIN ALTER THE RADIATION EFFECTS**

532 nm  rat myocardial  
cell  change in beating frequency<sup>39</sup>

**FIGURE 48.7** Experimental data obtained from irradiation of excitable cells indicating photoacceptors are located in the mitochondria.

distinct maxima in CD spectra (the spectra were recorded from 250 to 780 nm) of control cells were found at 566, 634, 680, 712, and 741 nm. After irradiation at 820 nm the most remarkable changes in peak positions as well as in CD signals were recorded in the range 750 to 770 nm — an appearance of a new peak at 767 nm and its shift to 757 nm after the second irradiation. Also, the peaks at 712 and 741 nm disappeared, and a new peak at 601 nm appeared. It was suggested that the changes in degree of oxidation of the chromophores of cytochrome *c* oxidase caused by the irradiation were accompanied by conformational changes in their vicinity. It was further suggested that these changes occurred in the environment of Cu<sub>B</sub>.<sup>33</sup> Even small structural changes in the binuclear site of cytochrome *c* oxidase control both rates of the dioxygen reduction and rates of internal electron- and proton-transfer reactions.<sup>29</sup>

The results of various studies<sup>27,28,32,33</sup> support the suggestion made earlier<sup>21</sup> that the mechanism of low-power laser therapy at the cellular level is based on the increase of oxidative metabolism in mitochondria, which is caused by electronic excitation of components of the respiratory chain (e.g., cytochrome *c* oxidase). Our results also provide evidence that various wavelengths (670, 632.8, and 820 nm) can be used for increasing respiratory activity. The wavelengths that were used in experiments described in References 27, 28, 32, and 33 were chosen in accordance with the maxima in the action spectra (Figure 48.4A and B). Note that 632.8 nm (He-Ne laser) and 820 nm (diode laser or LED) are the most common wavelengths used in therapeutic light sources.

It must be emphasized that when excitable cells (e.g., neurons, cardiomyocytes) are irradiated with monochromatic visible light, photoacceptors are also believed to be the components of the respiratory chain. Since the publication in 1947 of a study by Arvanitaki and Chalazonitis<sup>34</sup> it has been known that mitochondria of excitable cells have photosensitivity. Some of the experimental evidence concerning excitable cells is summarized briefly in Figure 48.7. These experiments were not performed in connection with light therapy. Experimental data<sup>35-39</sup> (see also Reference 40 and Chapter 5 of Reference 5) made it clear that monochromatic visible radiation could cause (via absorption in mitochondria) physiological and morphological changes in nonpigmented excitable cells, which do not contain specialized photoreceptors. Later, similar irradiation experiments were performed with neurons in connection with low-power laser therapy.<sup>5,40</sup> It was shown experimentally in the 1980s that He-Ne laser radiation altered the firing pattern of nerves. In addition, it was found that transcutaneous irradiation with a He-Ne laser mimicked the effect of peripheral stimulation of a behavioral reflex and that dose-related effects existed.<sup>41</sup> And, what is even more important, these findings were found to be connected with pain therapy.<sup>42,43</sup> Later clinical developments of these findings can be found in other publications.<sup>1,6,7</sup>

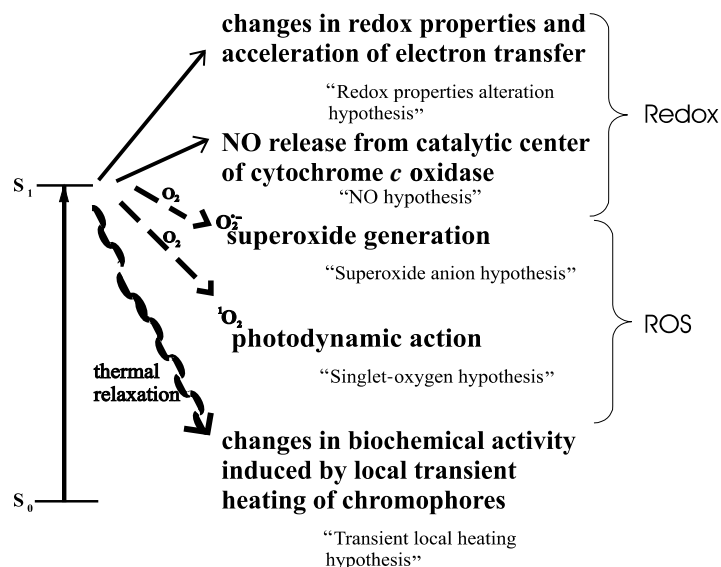


**FIGURE 48.8** Possible primary reactions in photoacceptor molecules after promotion of excited electronic states. ROS = reactive oxygen species.

### 48.3.2 Primary Reactions after Light Absorption

The primary mechanisms of light action after absorption of light quanta and the promotion of electronically excited states have not been established. The suggestions made to date are summarized in Figure 48.8; for simplicity, only singlet states ( $S_0$  and  $S_1$ ) are shown. However, triplet states are also involved.

Historically, the first mechanism, proposed in 1981 before recording of the action spectra, was the "singlet-oxygen hypothesis."<sup>44</sup> Certain photoabsorbing molecules like porphyrins and flavoproteins (some respiratory-chain components belong to these classes of compounds) can be reversibly converted to photosensitizers.<sup>45</sup> Based on visible-laser-light action on RNA synthesis rates in HeLa cells and spectroscopic data for porphyrins and flavins, the hypothesis was put forward that the absorption of light quanta by these molecules was responsible for the generation of singlet oxygen  $^1O_2$  and, therefore, for stimulation of the RNA-synthesis rate<sup>44</sup> and the DNA synthesis rate.<sup>9</sup> This possibility has been considered for some time as a predominant suppressive reaction when cells are irradiated at higher doses and intensities.<sup>3,5</sup>

The next mechanism proposed was the "redox properties alteration hypothesis" in 1988.<sup>21</sup> Photoexcitation of certain chromophores in the cytochrome *c* oxidase molecule (like  $Cu_A$  and  $Cu_B$  or hemes *a* and  $a_3$ )<sup>23</sup> influences the redox state of these centers and, consequently, the rate of electron flow in the molecule.<sup>21</sup>

The latest developments indicate that under physiological conditions the activity of cytochrome *c* oxidase is also regulated by nitric oxide (NO).<sup>46</sup> This regulation occurs via reversible inhibition of mitochondrial respiration. It was hypothesized<sup>47</sup> that laser irradiation and activation of electron flow in the molecule of cytochrome *c* oxidase could reverse the partial inhibition of the catalytic center by NO and in this way increase the  $O_2$ -binding and respiration rate ("NO hypothesis"). This may be a factor in the increase of the concentration of the oxidized form of  $Cu_B$  (Figure 48.5). Recent experimental results on the modification of irradiation effects with donors of NO do not exclude this hypothesis.<sup>48</sup> Note also that under pathological conditions the concentration of NO is increased (mainly due to the activation of macrophages producing NO<sup>49</sup>). This circumstance also increases the probability that the respiration activity of various cells will be inhibited by NO. Under these conditions, light activation of cell respiration may have a beneficial effect.

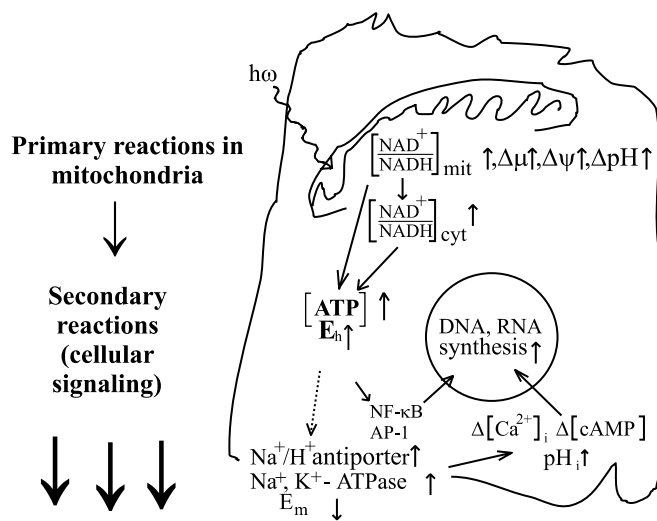


**FIGURE 48.9** Scheme of cellular signaling cascades (secondary reactions) occurring in a mammalian cell after primary reactions in the mitochondria.  $E_h \uparrow$  = shift of the cellular redox potential to more oxidized direction; the arrows  $\uparrow$  and  $\downarrow$  indicate increase or decrease of the respective values, brackets [ ] indicate the intracellular concentration of the respective chemicals.

When electronic states are excited with light, a noticeable fraction of the excitation energy is inevitably converted to heat, which causes a local transient increase in the temperature of absorbing chromophores (“transient local heating hypothesis”).<sup>50</sup> Any appreciable time- or space-averaged heating of the sample can be prevented by controlling the irradiation intensity and dose appropriately. The local transient rise in temperature of absorbing biomolecules may cause structural (e.g., conformational) changes and trigger biochemical activity (cellular signaling or secondary dark reactions).<sup>50,51</sup>

In 1993, it was suggested<sup>52</sup> that activation of the respiratory chain by irradiation would also increase production of superoxide anions (“superoxide anion hypothesis”). It has been shown that the production of  $O_2^-$  depends primarily on the metabolic state of the mitochondria.<sup>53</sup>

The belief that only one of the reactions discussed above occurs when a cell is irradiated and excited electronic states are produced is groundless. The question is, which mechanism is decisive? It is entirely possible that all the mechanisms discussed above lead to a similar result — a modulation of the redox state of the mitochondria (a shift in the direction of greater oxidation). However, depending on the light dose and intensity used, some of these mechanisms can prevail significantly. Experiments with *E. coli* provided evidence that, at different laser-light doses, different mechanisms were responsible — a photochemical one at low doses and a thermal one at higher doses.<sup>54</sup>

### 48.3.3 Cellular Signaling (Secondary Reactions)

If photoacceptors are located in the mitochondria, how then are the primary reactions that occur under irradiation in the respiratory chain connected with DNA and RNA synthesis in the nucleus (the action spectra in Figure 48.4A and B) or with changes in the plasma membrane (Figure 48.4C)? The principal answer is that between these events are secondary (dark) reactions (cellular signaling cascades or photo-signal transduction and amplification chain, Figure 48.9).

Figure 48.9 presents a possible scheme of cellular signaling cascades, which was first proposed to explain the increase in DNA synthesis rate after the irradiation of HeLa cells with monochromatic visible light.<sup>21</sup> New details have been added in recent years,<sup>5,22,25</sup> and the latest version of this scheme is presented in Figure 48.9.

Figure 48.9 suggests three regulation pathways. The first one is the control of the photoacceptor over the level of intracellular ATP. It is known that even small changes in ATP level can significantly alter cellular metabolism (55 for a review, see Reference). However, in many cases the regulative role of redox

homeostasis has proved to be more important than that of ATP. For example, the susceptibility of cells to hypoxic injury depends more on the capacity of cells to maintain the redox homeostasis and less on their capacity to maintain the energy status.<sup>56</sup>

The second and third regulation pathways are mediated through the cellular redox state. This may involve redox-sensitive transcription factors (NF- $\kappa$ B and AP-1 in Figure 48.9) or cellular signaling homeostatic cascades from cytoplasm via cell membrane to nucleus (Figure 48.9).<sup>3,21,22</sup> As a whole, the scheme in Figure 48.9 suggests a shift in overall cell redox potential in the direction of greater oxidation.

Recent experimental results of modification of an irradiation effect (increase of plasma-membrane adhesion when HeLa cells are irradiated at 820 nm) with various chemicals support the suggestions presented in Figure 48.9. Among these chemicals were respiratory-chain inhibitors,<sup>57</sup> donors of NO,<sup>58</sup> oxidants and antioxidants,<sup>57</sup> thiol reactive chemicals,<sup>58</sup> and chemicals that modify the activity of enzymes in the plasma membrane.<sup>59</sup> Recall that the overall redox state of a cell represents the net balance between stable and unstable reducing and oxidizing equivalents in dynamic equilibrium and is determined by three couples: NAD/NADH, NADP/NADPH, and GSH/GSSG (GSH = glutathione).

Recent studies have revealed that many cellular signaling pathways are regulated by the intracellular redox state (see References 60 through 63 for reviews). It is believed now that extracellular stimuli elicit cellular responses such as proliferation, differentiation, and even apoptosis through the pathways of cellular signaling. Modulation of the cellular redox state affects gene expression via mechanisms of cellular signaling (via effector molecules like transcription factors and phospholipase A<sub>2</sub>).<sup>60-62</sup> There are at least two well-defined transcription factors — nuclear factor kappa B (NF- $\kappa$ B) and activator protein (AP)-1 — that have been identified as being regulated by the intracellular redox state (see References 60 and 61 for reviews). As a rule, oxidants stimulate cellular signaling systems, and reductants generally suppress the upstream signaling cascades, resulting in suppression of transcription factors.<sup>64</sup> It is believed now that redox-based regulation of gene expression appears to represent a fundamental mechanism in cell biology.<sup>60,61</sup> It is important to emphasize that in spite of some similar or even identical steps in cellular signaling, the final cellular responses to irradiation can differ due to the existence of different modes of regulation of transcription factors.

It was suggested in 1988 that activation of cellular metabolism by monochromatic visible light was a redox-regulated phenomenon.<sup>21</sup> Specificity of the light action is as follows: the radiation is absorbed by the components of the respiratory chain, and this is the starting point for redox regulation. The experimental data from following years have supported this suggestion.

Dependencies of various biological responses (i.e., secondary reactions) on the irradiation dose, wavelength, pulsation mode, and intensity are available (for reviews, see References 2 through 5). The main features are mentioned here. Dose-biological response curves are usually bell-shaped, characterized by a threshold, a distinct maximum, and a decline phase. In most cases, the photobiological effects depend only on the radiation dose and not on the radiation intensity and exposure time (the reciprocity rule holds true), but in other cases the reciprocity rule proves invalid (the irradiation effects depend on light intensity). Although the biological responses of various cells may be qualitatively similar, they may have essential quantitative differences. The biological effects of irradiation depend on wavelength (action spectra). The biological responses of the same cells to pulsed and continuous-wave (CW) light of the same wavelength, average intensity, and dose can vary. (See Reference 5 for a detailed review).

Figure 48.10 explains magnitudes of low-power laser effects as being dependent on the initial redox status of a cell. The main idea expressed in Figure 48.10 is that cellular response is weak or absent (the dashed arrows on the right side) when the overall redox potential of a cell is optimal or near optimal for the particular growth conditions. The cellular response is stronger when the redox potential of the target cell is initially shifted (the arrows on left side) to a more reduced state (and intracellular pH,  $pH_i$ , is lowered). This explains why the degrees of cellular responses can differ markedly in different experiments and why they are sometimes nonexistent. A jump in  $pH_i$  due to irradiation has been measured experimentally (0.20 units in mammalian cells<sup>65</sup> and 0.32 units in *E. coli*<sup>66</sup>).

Various magnitudes of low-power laser effects (strong effect, weak effect, or no effect at all) have always been one of the most criticized aspects of low-power laser therapy. An attempt was made to quantify the

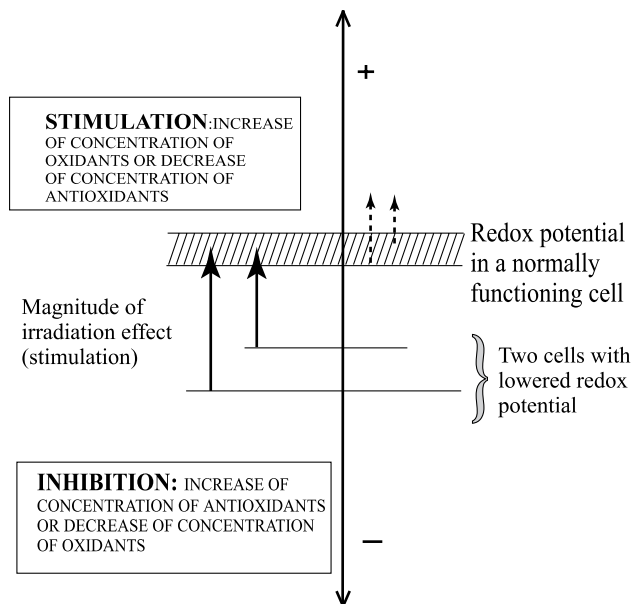


**FIGURE 48.10** Schematic illustration of the action principle of monochromatic visible and NIR radiation on a cell. Irradiation shifts the cellular redox potential in a more oxidized direction. The magnitude of cellular response is determined by the cellular redox potential at the moment of irradiation.

magnitude of irradiation effects as dependent on the metabolic status of *E. coli* cells<sup>67</sup> (for a review, see Reference 26). Recently, the correlation was found between the amount of ATP in irradiated cells and the initial amount of ATP in control cells.<sup>68</sup>

Thus, variations in the magnitude of low-power laser effects at the cellular level are explained by the overall redox state (and  $pH_i$ ) at the moment of irradiation. Cells with a lowered  $pH_i$  (in which redox state is shifted to the reduced side) respond stronger than cells with a normal or close-to-normal  $pH_i$  value.

#### 48.3.4 Partial Derepression of Genome of Human Peripheral Lymphocytes: Biological Limitations of Low-Power Laser Effects

Monochromatic visible light cannot always induce full metabolic activation. One such example is considered in this section. Circulating lymphocytes confronted with an immunological stimulus shift from the resting state ( $G_0$ -phase of cellular cycle) to one of rapid enlargement, culminating in DNA synthesis and mitosis (blast transformation). The characteristics of biochemical and morphological reactions in lymphocytes under the action of mitogens (agents responsible for blast transformation, e.g., phytohemagglutinin, [PHA]) have been studied for years (for a review, see Reference 69). Cellular responses to a mitogen can be divided into short-term responses without *de novo* protein synthesis and occurring during the first seconds, minutes, and hours after contact with the mitogen starts and long-term ones connected with protein synthesis hours and days after the beginning of stimulation.

Parallel experiments with PHA treatment and He-Ne laser irradiation were carried out, and the results for these two experimental groups were compared with each other and with those of intact control.<sup>70-76</sup> The 10-sec irradiation with a He-Ne laser ( $D = 56 \text{ J/m}^2$ ) induced short-term changes in lymphocytes that were qualitatively similar and quantitatively close to those caused by PHA (which is present in the incubation medium during all experiments). Among short-term responses compared in this set of experiments were  $\text{Ca}^{2+}$  influx, RNA synthesis, accessibility of chromatin to acridine orange (a test characterizing the chromatin template activity and its transcription function), and steady-state level of *c-myc* mRNA.<sup>70-73</sup> Also, ultrastructural changes of the nucleus<sup>74</sup> and chromatin<sup>75</sup> were found to be similar in



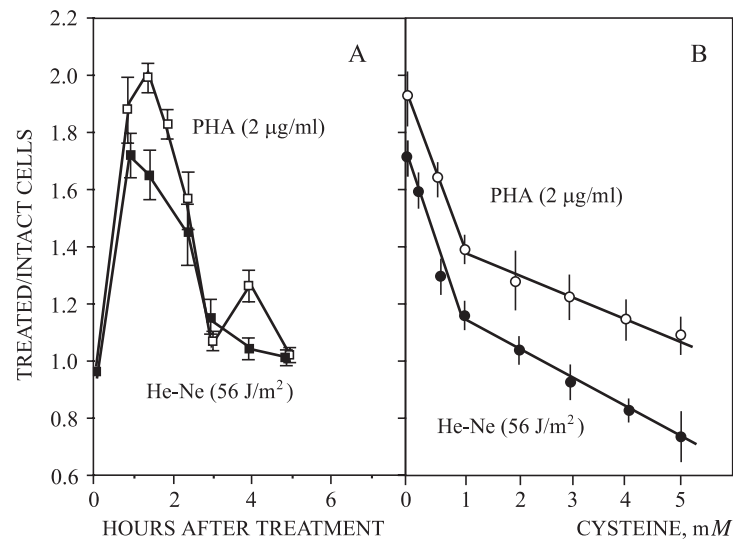


**FIGURE 48.11** Transcription activation (measured by binding of acridine orange to chromatin) of human peripheral lymphocytes: (A) after irradiation with He-Ne laser (10 sec,  $56 \text{ J/m}^2$ ) or treatment with phytohemagglutinin (PHA,  $2 \mu\text{g/ml}$ ); (B) decrease of transcription activation 1 h after irradiation or PHA treatment depending on concentration of cysteine added immediately after the irradiation or adding PHA. (Modified from Fedoseyeva, G.E. et al., *Lasers Life Sci.*, 2, 197, 1988.)

two experimental groups during the first hours after stimulation. These changes were interpreted as an activation of rRNA metabolism, including its synthesis, processing, and transport.<sup>74</sup>

Two characteristic features of laser-light action were established. First, transcription function was activated in T-lymphocytes but not in B-lymphocytes. At the same time, PHA was stimulative for both types of lymphocytes.<sup>76</sup> Second, despite the similarities in the early responses of lymphocytes to PHA and He-Ne laser radiation, the irradiated lymphocytes did not enter the S-phase of the cell cycle.<sup>71,72</sup> This means that full mitogenic activation did not occur in the irradiated lymphocytes. It is quite possible that the period of irradiation (10 sec in our experiments) was too short to cause the entire cascade of reactions needed for blast transformation. But this time was long enough to cause a boosting effect of blast transformation in PHA-treated lymphocytes.<sup>71,72</sup> The number of blast-transformed cells in the sample, which was irradiated before the beginning of PHA treatment, was 120 to 170% higher depending on PHA concentration.<sup>71,72</sup> It was suggested that the cause of this effect was a partial activation of lymphocytes under irradiation.<sup>71</sup> This may also be a conditioning (priming) effect of certain subpopulations of lymphocytes.<sup>47</sup> It is possible that this is a redox priming effect. Two lines of evidence allow for this suggestion.

First, it is believed that lymphocyte activation under laser radiation starts with mitochondria, as described in Section 48.3.1. This suggestion is supported by experiments showing that ATP extrasynthesis and an increase of energy charge occur in irradiated lymphocytes.<sup>77</sup> Formation of giant mitochondrial structures in the irradiated cells indicated that a higher level of respiration and energy turnover occurred in these cells.<sup>78</sup> But recording of action spectra is needed for further studies of photoacceptors in lymphocytes.

Second, the early transcriptional activation of lymphocytes both by PHA and He-Ne laser radiation (Figure 48.11A) can be eliminated by a reducing agent, cysteine (Figure 48.11B).<sup>70</sup> As seen in Figure 48.11B, the effect depends on the concentration of cysteine. Cysteine also cancels blast transformation of lymphocytes.<sup>79</sup> The activation events in T-lymphocytes and monocytes, which are mediated through translocation of the transcription factor NF- $\kappa$ B, depend on the redox state of these cells.<sup>80</sup> A basal redox equilibrium tending toward oxidation was a prerequisite for the activation of T-lymphocytes

and U937 monocytes; both constitutive activation as well as that induced by mitogens were inhibited or even canceled by treatment of cells with reducing agents or antioxidants.<sup>79,80</sup>

Partial mitogenic activation of lymphocytes under He-Ne laser radiation is not the only example of limited activation. For example, silent neurons of *Helix pomatia* did not respond to He-Ne laser irradiation, while the spontaneously active neurons responded strongly under the same experimental conditions.<sup>40</sup> Only 25 to 27% of 3T3 fibroblasts responded to NIR radiation by extending their pseudopodia toward the monochromatic-light source.<sup>81</sup>

The results of experiments with *E. coli* batches showed that they contained a subpopulation that, in response to the irradiation, rapidly began a new cycle of replication and division.<sup>5,26</sup> The number of cells in this subpopulation depended on the cultivation conditions, being smaller in faster-growing populations (e.g., the glucose-grown culture) and larger in slower-growing populations (e.g., the arabinose-grown culture). Presumably, in cells of this light-sensitive subpopulation, the particular metabolic state necessary for the division could be established. Irradiation is what enables the cells to achieve this active state rapidly. Also, this set of experiments<sup>5,26</sup> clearly proved that there is a limit to the specific growth rate of all populations ( $0.80 \text{ h}^{-1}$ ) that does not depend on growth conditions, and in addition that populations that are already growing at this rate cannot be stimulated. This was also found to be the reason why *E. coli* growth was maximally stimulated not in summer but rather in winter. In autumn and winter, the intact culture featured relatively slow growth. In spring and summer, when the growth of that culture accelerated and the growth rate of the control culture was almost comparable to that of the culture exposed to the optimum dose of red light in the autumn-winter period, irradiation had but little effect.<sup>3</sup>

One conclusion from experiments with cultured cells was that only proliferation of slowly growing subpopulations could be stimulated by irradiation. Also, the experiments with HeLa cells demonstrated that one of the effects of He-Ne laser irradiation of these cells was a decrease of the duration of the  $G_1$  period but not other periods of the cell cycle<sup>82</sup> (for a review, see Reference 83).

Taken together, there exist certain biological as well as other limitations connected with the physiological status of an irradiated object.

#### 48.4 Enhancement of Cellular Metabolism via Activation of Nonmitochondrial Photoacceptors: Indirect Activation/Suppression

The redox-regulation mechanism cannot occur solely via the respiratory chain (see Section 48.3). Redox chains containing molecules that absorb light in the visible spectral region are usually key structures that can regulate metabolic pathways. One such example is NADPH-oxidase of phagocytic cells, which is responsible for nonmitochondrial respiratory burst. This multicomponent enzyme system is a redox chain that generates reactive oxygen species (ROS) as a response to the microbicidal or other types of activation. Irradiation with the He-Ne<sup>84-87</sup> and semiconductor lasers and LEDs<sup>52,88-91</sup> can activate this chain. The features of radiation-induced nonmitochondrial respiratory burst, which was quantitatively and qualitatively characterized by measurements of luminol-amplified chemiluminescence (CL),<sup>84-91</sup> must be followed. First, nonmitochondrial respiratory burst can be induced both in homogeneous cell populations and cellular systems (blood, spleen cells, and bone marrow) by both CW and pulsed lasers and LEDs. Figure 48.12 presents some examples. Qualitatively, the kinetics of CL enhancement after irradiation is similar to that after treatment of cells with an object of phagocytosis, *Candida albicans*. Quantitatively, the intensity of induced by radiation CL is approximately one order of magnitude lower (Figure 48.12B). This is true for He-Ne laser radiation<sup>84</sup> as well as for radiation of various pulsed LEDs.<sup>88,91</sup> Second, irradiation effects (stimulation or inhibition of CL) on phagocytic cells strongly depend on the health status of the host organism.<sup>85-90</sup> This circumstance can be used for diagnostic purposes. Third, there are complex dependencies on irradiation parameters; irradiation can suppress or activate the nonmitochondrial respiratory burst.<sup>88-91</sup> These problems have been reviewed in detail elsewhere.<sup>5</sup>

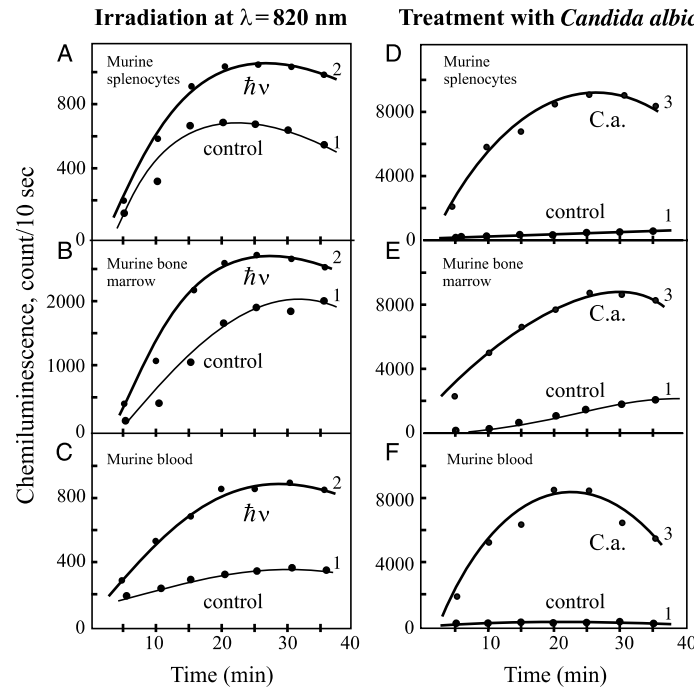


**FIGURE 48.12** Kinetic curves of chemiluminescence of murine splenocytes (A, D), bone marrow (B, E), and blood (C, F) after irradiation (A–C) or treatment (D–F) with *Candida albicans*. Curve 1 denotes everywhere the spontaneous chemiluminescence of control cells; curve 2 is chemiluminescence after irradiation of samples in dose  $800 \text{ J/m}^2$  ( $I = 51 \text{ W/m}^2$ ,  $f = 292 \text{ Hz}$ ); and curve 3 marks the chemiluminescence induced by the treatment with *C. albicans* ( $5 \times 10^7$  particles/ml). The measurement error is  $\leq \pm 5\%$ . (From Karu, T.I. et al., *Lasers Surg. Med.*, 21, 485, 1997.)

Finally, reactive-oxygen species, the burst of which is induced by direct irradiation of phagocytes, can activate or deactivate other cells that were not directly irradiated. In this way, indirect activation (or suppression) of metabolic pathways in nonirradiated cells occurs. Cooperative action among various cells via secondary messengers (ROS, lymphokines, cytokines,<sup>92</sup> and NO<sup>93</sup>) requires much more attention when the mechanisms of low-power laser therapy are considered at the organism level.

This chapter did not consider systemic effects of low-power laser therapy at the organism level. The mechanisms of these effects have not yet been established. Perhaps NO plays a role as a secondary messenger for systemic effects of laser irradiation. A possible mechanism connected with the NO-cytochrome *c* oxidase complex was considered earlier (Section 48.3.2). In addition, mechanisms of analgesic effects of laser radiation<sup>94</sup> and systemic therapeutic effects that occur via blood irradiation<sup>95</sup> could be connected with NO.

Recent studies have demonstrated that a number of nonphagocytic cell types, including fibroblasts, osteoblasts, endothelial cells, chondrocytes, kidney mesangial cells, and others, generate ROS (mainly superoxide anion) in low concentrations in response to stimuli.<sup>96</sup> The function of this ROS production is not yet known. It is believed that an NADPH-oxidase (probably different from that in phagocytic cells) is present in nonphagocytic cells as well.<sup>96</sup> To date, the effects of irradiation on this enzyme have not yet been studied.

Another example of important redox chains are NO-synthases, a group of redox-active P450-like flavocytochromes that are responsible for NO generation under physiological conditions.<sup>97</sup> So far, the irradiation effects on these systems have not been investigated.

## 48.5 Conclusion

This chapter considered three principal ways of activating individual cells by monochromatic (laser) light. The photobiological action mechanism via activation of the respiratory chain is a universal mechanism. Primary photoacceptors are terminal oxidases (cytochrome *c* oxidase in eukaryotic cells and, for example, cytochrome *bd* complex in the prokaryotic cell of *E. coli*) as well as NADH-dehydrogenase (for the blue-to-red spectral range). Primary reactions in or with a photoacceptor molecule lead to photobiological responses at the cellular level through cascades of biochemical homeostatic reactions (cellular signaling or photosignal transduction and amplification chain). Crucial events of this type of cell-metabolism activation occur due to a shift of cellular redox potential in the direction of greater oxidation. Cell-metabolism activation via the respiratory chain occurs in all cells susceptible to light irradiation. Susceptibility to irradiation and capability for activation depend on the physiological status of irradiated cells; cells whose overall redox potential is shifted to a more reduced state (e.g., certain pathological conditions) are more sensitive to irradiation. The specificity of final photobiological response is determined not at the level of primary reactions in the respiratory chain but at the transcription level during cellular signaling cascades. In some cases, only partial activation of cell metabolism happens (e.g., priming of lymphocytes). All light-induced biological effects depend on the parameters of the irradiation (wavelength, dose, intensity, radiation time, CW or pulsed mode, pulse parameters).

Other redox chains in cells can also be activated by irradiation. In phagocytic cells irradiation initiates a nonmitochondrial respiratory burst (production of reactive oxygen species, especially superoxide anion) through activation of NADPH-oxidase located in the plasma membrane of these cells. The irradiation effects on phagocytic cells depend on the physiological status of the host organism as well as on radiation parameters.

Direct activation of cells can lead to the indirect activation of other cells. This occurs via secondary messengers released by directly activated cells: reactive oxygen species produced by phagocytes, lymphokines and cytokines produced by various subpopulations of lymphocytes, or NO produced by macrophages or as a result of NO-hemoglobin photolysis of red blood cells.

Coherent properties of laser light are not manifested at the molecular level by light interaction with biotissue. The absorption of low-intensity laser light by biological systems is of a purely noncoherent (i.e., photobiological) nature. At the cellular level, biological responses are determined by absorption of light with photoacceptor molecules. Coherent properties of laser light are unimportant when the cellular monolayer, the thin layer of cell suspension, and the thin layer of tissue surface are irradiated. In these cases, the coherent and noncoherent light with the same wavelength, intensity, and dose provides the same biological response. Some additional (therapeutic) effects from coherent and polarized radiation can occur only in deeper layers of bulk tissue.

## Acknowledgments

I am indebted to Prof. V.S. Letokhov for helpful comments and discussions about the effects of coherent and noncoherent light. Partial financial support from the Ministry of Science, Industry, and Technology of the Russian Federation (grant 108-12(00)) and the Ministry of Science and Technology of the Moscow Region and Russian Foundation of Basic Research (grant 01-02-97025) are acknowledged.

## References

1. Tuner, J. and Hode, L., *Low Level Laser Therapy: Clinical Practice and Scientific Background*, Prima Books, Grängesberg, Sweden, 1999.
2. Karu, T.I., Photobiological fundamentals of low-power laser therapy, *IEEE J. Quantum Electron.*, QE-23, 1703, 1987.
3. Karu, T.I., *Photobiology of Low-Power Laser Therapy*, Harwood Academic, London, 1989.

4. Karu, T.I., Photobiology of low-power laser effects, *Health Phys.*, 56, 691, 1989.
5. Karu, T., *The Science of Low Power Laser Therapy*, Gordon & Breach, London, 1998.
6. Baxter, G.D., *Therapeutic Lasers: Theory and Practice*, Churchill Livingstone, London, 1994.
7. Simunovic, Z., Ed., *Lasers in Medicine and Dentistry*, Vitgraf, Rijeka (Croatia), 2000.
8. Sazonov, A.M., Romanov, G.A., Portnoy, L.M., Odinkova, V.A., Karu, T.I., Lobko, V.V., and Letokhov, V.S., Low-intensity noncoherent red light in complex healing of peptic and duodenal ulcers, *Sov. Med.*, 12, 42, 1985 (in Russian).
9. Karu, T.I., Kalendo, G.S., Letokhov, V.S., and Lobko, V.V., Biostimulation of HeLa cells by low intensity visible light, *Nuov. Cim. D*, 1, 828, 1982.
10. Karu, T.I., Tiphlova, O.A., Letokhov, V.S., and Lobko, V.V., Stimulation of *E. coli* growth by laser and incoherent red light, *Nuov. Cim. D*, 2, 1138, 1983.
11. Bertoloni, G., Sacchetto, R., Baro, E., Ceccherelli, F., and Jori, G., Biochemical and morphological changes in *Escherichia coli* irradiated by coherent and non-coherent 632.8 nm light, *J. Photochem. Photobiol. B Biol.*, 18, 191, 1993.
12. Hartman, K.M., Action spectroscopy, in *Biophysics*, Hoppe, W., Lohmann, W., Marke, H., and Ziegler, H., Eds., Springer-Verlag, Heidelberg, 1983, p. 115.
13. Lipson, E.D., Action spectroscopy: methodology, in *CRC Handbook of Organic Chemistry and Photobiology*, Horspool, W.H. and Song, P.-S., Eds., CRC Press, Boca Raton, FL, 1995, p. 1257.
14. Karu, T.I., Kalendo, G.S., Letokhov, V.S., and Lobko, V.V., Biological action of low-intensity visible light on HeLa cells as a function of the coherence, dose, wavelength, and irradiation dose, *Sov. J. Quantum Electron.*, 12, 1134, 1982.
15. Karu, T.I., Kalendo, G.S., Letokhov, V.S., and Lobko, V.V., Biological action of low-intensity visible light on HeLa cells as a function of the coherence, dose, wavelength, and irradiation regime. II., *Sov. J. Quantum Electron.*, 13, 1169, 1983.
16. Karu, T.I., Tiphlova, O.A., Fedoseyeva, G.E., Kalendo, G.S., Letokhov, V.S., Lobko, V.V., Lyapunova, T.S., Pomoshnikova, N.A., and Meissel, M.N., Biostimulating action of low-intensity monochromatic visible light: is it possible? *Laser Chem.*, 5, 19, 1984.
17. Gamaleya, N.F., Shishko, E.D., and Yanish, G.B., New data about mammalian cells photosensitivity and laser biostimulation, *Dokl. Akad. Nauk S.S.S.R. (Moscow)*, 273, 224, 1983.
18. Vekshin, N.A., Light-dependent ATP synthesis in mitochondria, *Mol. Biol. (Moscow)*, 25, 54, 1991.
19. Karu, T.I., Kalendo, G.S., Letokhov, V.S., and Lobko, V.V., Biostimulation of HeLa cells by low-intensity visible light. II. Stimulation of DNA and RNA synthesis in a wide spectral range, *Nuov. Cim. D*, 3, 309, 1984.
20. Karu, T.I., Kalendo, G.S., Letokhov, V.S., and Lobko, V.V., Biostimulation of HeLa cells by low intensity visible light. III. Stimulation of nucleic acid synthesis in plateau phase cells, *Nuov. Cim. D*, 3, 319, 1984.
21. Karu, T.I., Molecular mechanism of the therapeutic effect of low-intensity laser radiation, *Lasers Life Sci.*, 2, 53, 1988.
22. Karu, T., Primary and secondary mechanisms of action of visible-to-near IR radiation on cells, *J. Photochem. Photobiol. B Biol.*, 49, 1, 1999.
23. Karu, T.I. and Afanasyeva, N.I., Cytochrome oxidase as primary photoacceptor for cultured cells in visible and near IR regions, *Dokl. Akad. Nauk (Moscow)*, 342, 693, 1995.
24. Karu, T.I., Pyatibrat, L.V., Kalendo, G.S., and Esenaliev, R.O., Effects of monochromatic low-intensity light and laser irradiation on adhesion of HeLa cells *in vitro*, *Lasers Surg. Med.*, 18, 171, 1996.
25. Karu, T., Low-power laser effects, in *Lasers in Medicine*, Waynant, R., Ed., CRC Press, Boca Raton, FL, 2002, p. 169.
26. Tiphlova, O. and Karu, T., Action of low-intensity laser radiation on *Escherichia coli*, *CRC Critical Rev. Biomed. Eng.*, 18, 387, 1991.

27. Karu, T.I., Afanasyeva, N.I., Kolyakov, S.F., and Pyatibrat, L.V., Changes in absorption spectra of monolayer of living cells after irradiation with low intensity laser light, *Dokl. Akad. Nauk (Moscow)*, 360, 267, 1998.
28. Karu, T.I., Afanasyeva, N.I., Kolyakov, S.F., Pyatibrat, L.V., and Welser, L., Changes in absorbance of monolayer of living cells induced by laser radiation at 633, 670, and 820 nm, *IEEE J. Sel. Top. Quantum Electron.*, 7, 982, 2001.
29. Jöbbsis-van der Vliet, F.F., Discovery of the near-infrared window in the body and the early development of near-infrared spectroscopy, *J. Biomed. Opt.*, 4, 392, 1999.
30. Jöbbsis-van der Vliet, F.F. and Jöbbsis, P.D., Biochemical and physiological basis of medical near-infrared spectroscopy, *J. Biomed. Opt.*, 4, 397, 1999.
31. Dube, A., Gupta, P.K., and Bharti, S., Redox absorbance changes of the respiratory chain components of *E. coli* following He-Ne laser irradiation, *Lasers Life Sci.*, 7, 173, 1997.
32. Kolyakov, S.F., Pyatibrat, L.V., Mikhailov, E.L., Kompanets, O.N., and Karu, T.I., Changes in the spectra of circular dichroism of suspension of living cells after low intensity laser radiation at 820 nm, *Dokl. Akad. Nauk (Moscow)*, 377, 824, 2001.
33. Karu, T.I., Kolyakov, S.F., Pyatibrat, L.V., Mikhailov, E.L., and Kompanets, O.N., Irradiation with a diode at 820 nm induces changes in circular dichroism spectra (250–750 nm) of living cells, *IEEE J. Sel. Top. Quantum Electron.*, 7, 976, 2001.
34. Arvanitaki, A. and Chalazonitis, N., Reactions bioelectriques a la photoactivation des cytochromes, *Arch. Sci. Physiol.*, 1, 385, 1947.
35. Berns, M.W., Gross, D.C.L., Cheng, W.K., and Woodring, D., Argon laser microirradiation of mitochondria in rat myocardial cell in tissue culture. II. Correlation of morphology and function in single irradiated cells, *J. Mol. Cell. Cardiol.*, 4, 71, 1972.
36. Berns, M.W. and Salet, C., Laser microbeam for partial cell irradiation, *Int. Rev. Cytol.*, 33, 131, 1972.
37. Salet, C., Acceleration par micro-irradiation laser du rythme de contraction de cellular cardiaques en culture, *C.R. Acad. Sci. Paris*, 272, 2584, 1971.
38. Salet, C., A study of beating frequency of a single myocardial cell. I. Q-switched laser microirradiation of mitochondria, *Exp. Cell Res.*, 73, 360, 1972.
39. Salet, C., Moreno, G., and Vinzens, F., A study of beating frequency of a single myocardial cell. III. Laser microirradiation of mitochondria in the presence of KCN or ATP, *Exp. Cell Res.*, 120, 25, 1979.
40. Balaban, P., Esenaliev, R., Karu, T., Kutomkina, E., Letokhov, V., Oraevsky, A., and Ovcharenko, N., He-Ne laser irradiation of single identified neurons, *Lasers Surg. Med.*, 12, 329, 1992.
41. Walker, J. and Akhanjee, K., Laser-induced somatosensory evoked potential: evidence of photosensitivity of peripheral nerves, *Brain Res.*, 344, 281, 1985.
42. Walker, J., Relief from chronic pain by laser irradiation, *Neurosci. Lett.*, 43, 339, 1983.
43. Walker, J., Treatment of human neurological problems by laser photostimulation, U.S. patent 4,671,285, 1987.
44. Karu, T.I., Kalendo, G.S., and Letokhov, V.S., Control of RNA synthesis rate in tumor cells HeLa by action of low-intensity visible light of copper laser, *Lett. Nuov. Cim.*, 32, 55, 1981.
45. Giese, A.C., Photosensitization of organisms with special reference to natural photosensitizers, in *Lasers in Biology and Medicine*, Hillenkampf, F., Pratesi, R., and Sacchi, C., Eds., Plenum Press, New York, 1980, p. 299.
46. Brown, G.C., Nitric oxide and mitochondrial respiration, *Biochem. Biophys. Acta*, 1411, 351, 1999.
47. Karu, T., Mechanisms of low-power laser light action on cellular level, in *Lasers in Medicine and Dentistry*, Simunovic, Z., Ed., Vitgraf, Rijeka (Croatia), 2000, p. 97.
48. Karu, T.I., Pyatibrat, L.V., and Kalendo, G.S., Donors of NO and pulsed radiation at  $\lambda=820$  nm exert effects on cells attachment to extracellular matrices, *Toxicol. Lett.*, 121, 57, 2001.
49. Hothersall, J.S., Cunha, F.Q., Neild, G.H., and Norohna-Dutra, A., Induction of nitric oxide synthesis in J774 cell lowers intracellular glutathione: effect of oxide modulated glutathione redox status on nitric oxide synthase induction, *Biochem. J.*, 322, 477, 1997.

50. Karu, T.I., Tiphlova, O.A., Matveyets, Yu. A., Yartsev, A.P., and Letokhov, V.S., Comparison of the effects of visible femtosecond laser pulses and continuous wave laser radiation of low average intensity on the clonogenicity of *Escherichia coli*, *J. Photochem. Photobiol. B Biol.*, 10, 339, 1991.
51. Karu, T.I., Local pulsed heating of absorbing chromophores as a possible primary mechanism of low-power laser effects, in *Laser Applications in Medicine and Surgery*, Galletti, G., Bolognani, L., and Ussia, G., Eds., Monduzzi Editore, Bologna, 1992, p. 253.
52. Karu, T., Andreichuk, T., and Ryabykh, T., Changes in oxidative metabolism of murine spleen following diode laser (660–950nm) irradiation: effect of cellular composition and radiation parameters, *Lasers Surg. Med.*, 13, 453, 1993.
53. Forman, N.J. and Boveris, A., Superoxide radical and hydrogen peroxide in mitochondria, in *Free Radicals in Biology*, Vol. 5, Pryor, A., Ed., Academic Press, New York, 1982, p. 65.
54. Karu, T., Tiphlova, O., Esenaliev, R., and Letokhov, V., Two different mechanisms of low-intensity laser photobiological effects on *Escherichia coli*, *J. Photochem. Photobiol. B Biol.*, 24, 155, 1994.
55. Brown, G.C., Control of respiration and ATP synthesis in mammalian mitochondria and cells, *Biochem. J.*, 284, 171, 1992.
56. Chance, B., Cellular oxygen requirements, *Fed. Proc. Fed. Am. Soc. Exp. Biol.*, 16, 671, 1957.
57. Karu, T.I., Pyatibrat, L.V., and Kalendo, G.S., Cell attachment modulation by radiation from a pulsed semiconductor light diode ( $\lambda=820$  nm) and various chemicals, *Lasers Surg. Med.*, 28, 227, 2001.
58. Karu, T.I., Pyatibrat, L.V., and Kalendo, G.S., Thiol reactive agents and semiconductor light diode radiation ( $\lambda=820$  nm) exert effects on cell attachment to extracellular matrix, *Laser Ther.*, 11, 177, 2001.
59. Karu, T.I., Pyatibrat, L.V., and Kalendo, G.S., Cell attachment to extracellular matrices is modulated by pulsed radiation at 820 nm and chemical that modify the activity of enzymes in the plasma membrane, *Lasers Surg. Med.*, 29, 274, 2001.
60. Gius, D., Boreto, A., Shah, S., and Curry, H.A., Intracellular oxidation reduction status in the regulation of transcription factors NF- $\kappa$ B and AP-1, *Toxicol. Lett.*, 106, 93, 1999.
61. Sun, Y. and Oberley, L.W., Redox regulation of transcriptional activators, *Free Rad. Biol. Med.*, 21, 335, 1996.
62. Nakamura, H., Nakamura, K., and Yodoi, J., Redox regulation of cellular activation, *Annu. Rev. Immunol.*, 15, 351, 1997.
63. Kamata, H. and Hirata, H., Redox regulation of cellular signalling, *Cell. Signal.*, 11, 1, 1999.
64. Calkhoven, C.F. and Geert, A.B., Multiple steps in regulation of transcription-factor level and activity, *Biochemistry*, 317, 329, 1996.
65. Chopp, H., Chen, Q., Dereski, M.O., and Hetzel, F.W., Chronic metabolic measurement of normal brain tissue response to photodynamic therapy, *Photochem. Photobiol.*, 52, 1033, 1990.
66. Quickenden, T.R., Daniels, L.L., and Byrne, L.T., Does low-intensity He-Ne radiation affect the intracellular pH of intact *E. coli*? *Proc. SPIE*, 2391, 535, 1995.
67. Tiphlova, O. and Karu, T., Dependence of *Escherichia coli* growth rate on irradiation with He-Ne laser and growth substrates, *Lasers Life Sci.*, 4, 161, 1991.
68. Karu, T.I., Pyatibrat, L.V., and Kalendo, G.S., Studies into the action specifics of a pulsed GaAlAs laser ( $\lambda=820$  nm) on a cell culture. I. Reduction of the intracellular ATP concentration: dependence on initial ATP amount, *Lasers Life Sci.*, 9, 203, 2001.
69. Ashman, R.F., Lymphocyte activation, in *Fundamental Immunology*, Paul, W.P., Ed., Raven Press, New York, 1984, p. 267.
70. Fedoseyeva, G.E., Smolyaninova, N.K., Karu, T.I., and Zelenin, A.V., Human lymphocyte chromatin changes following irradiation with a He-Ne laser, *Lasers Life Sci.*, 2, 197, 1988.
71. Karu, T.I., Smolyaninova, N.K., and Zelenin, A.V., Long-term and short-term responses of human lymphocytes to He-Ne laser radiation, *Lasers Life Sci.*, 4, 167, 1991.

72. Smolyaninova, N.K., Karu, T.I., Fedoseyeva, G.E., and Zelenin, A.V., Effect of He-Ne laser irradiation on chromatin properties and nucleic acids synthesis of human blood lymphocytes, *Biomed. Sci.*, 2, 121, 1991.
73. Shliakhova, L.N., Itkes, A.V., Manteifel, V.M., and Karu, T.I., Expression of *c-myc* gene in irradiated at 670 nm human lymphocytes: a preliminary report, *Lasers Life Sci.*, 7, 107, 1996.
74. Manteifel, V.M. and Karu, T.I., Ultrastructural changes in human lymphocytes under He-Ne laser radiation, *Lasers Life Sci.*, 4, 235, 1992.
75. Manteifel, V.M., Andreichuk, T.N., and Karu, T.I., Influence of He-Ne laser radiation and phytohemagglutinin on the ultrastructure of chromatin of human lymphocytes, *Lasers Life Sci.*, 6, 1, 1994.
76. Manteifel, V.M. and Karu, T.I., Activation of chromatin in T-lymphocytes nuclei under the He-Ne laser radiation, *Lasers Life Sci.*, 8, 117, 1998.
77. Herbert, K.E., Bhusate, L.L., Scott, D.L., Diamantopolos, C., and Perrett, D., Effect of laser light at 820 nm on adenosine nucleotide levels in human lymphocytes, *Lasers Life Sci.*, 3, 37, 1989.
78. Manteifel, V., Bakeeva, L., and Karu, T., Ultrastructural changes in chondriome of human lymphocytes after irradiation with He-Ne laser: appearance of giant mitochondria, *J. Photochem. Photobiol. B Biol.*, 38, 25, 1997.
79. Novogrodski, A., Lymphocyte activation induced by modifications of surface, in *Immune Recognition*, Rosenthal, S., Ed., Academic Press, New York, 1975, p. 43.
80. Israël, N., Gougerot-Pocidallo, M.-A., Aillet, F., and Verelizier, J.-L., Redox status of cells influences constitutive or induced NF- $\kappa$ B translocation and HIV long terminal repeat activity in human T-lymphocytes and monocytic cell lines, *J. Immunol.*, 149, 3386, 1992.
81. Albrecht-Büchler, G., Surface extensions of 3T3 cells towards distant infrared light sources, *J. Cell Biol.*, 114, 494, 1991.
82. Karu, T.I., Pyatibrat, L.V., and Kalendo, G.S., Biostimulation of HeLa cells by low-intensity visible light. V. Stimulation of cell proliferation *in vitro* by He-Ne laser radiation, *Nuov. Cim. D*, 9, 1485, 1987.
83. Karu, T., Effects of visible radiation on cultured cells, *Photochem. Photobiol.*, 52, 1089, 1090.
84. Karu, T.I., Ryabykh, T.P., Fedoseyeva, G.E., and Puchkova, N.I., Induced by He-Ne laser radiation respiratory burst on phagocytic cells, *Lasers Surg. Med.*, 9, 585, 1989.
85. Karu, T.I., Ryabykh, T.P., and Antonov, S.N., Different sensitivity of cells from tumor-bearing organisms to continuous-wave and pulsed laser radiation ( $\lambda = 632.8$  nm) evaluated by chemiluminescence test. I. Comparison of responses of murine splenocytes: intact mice and mice with transplanted leukemia EL-4, *Lasers Life Sci.*, 7, 91, 1996.
86. Karu, T.I., Ryabykh, T.P., and Antonov, S.N., Different sensitivity of cells from tumor-bearing organisms to continuous-wave and pulsed laser radiation ( $\lambda = 632.8$  nm) evaluated by chemiluminescence test. II. Comparison of responses of human blood: healthy persons and patients with colon cancer, *Lasers Life Sci.*, 7, 99, 1996.
87. Karu, T.I., Ryabykh, T.P., and Letokhov, V.S., Different sensitivity of cells from tumor-bearing organisms to continuous-wave and pulsed laser radiation ( $\lambda = 632.8$  nm) evaluated by chemiluminescence test. III. Effect of dark period between pulses, *Lasers Life Sci.*, 7, 141, 1997.
88. Karu, T., Andreichuk, T., and Ryabykh, T., Suppression of human blood chemiluminescence by diode laser radiation at wavelengths 660, 820, 880 or 950 nm, *Laser Ther.*, 5, 103, 1993.
89. Karu, T.I., Andreichuk, T.N., and Ryabykh, T.P., On the action of semiconductor laser radiation ( $\lambda = 820$  nm) on the chemiluminescence of blood of clinically healthy humans, *Lasers Life Sci.*, 6, 277, 1995.
90. Karu, T.I., Ryabykh, T.P., Sidorova, T.A., and Dobrynin, Ya.V., The use of a chemiluminescence test to evaluate the sensitivity of blast cells in patients with hemoblastoses to antitumor agents and low-intensity laser radiation, *Lasers Life Sci.*, 7, 1, 1996.
91. Karu, T.I., Pyatibrat, L.V., and Ryabykh, T.P., Nonmonotonic behaviour of the dose dependence of the radiation effect on cells *in vitro* exposed to pulsed laser radiation at  $\lambda = 820$  nm, *Lasers Surg. Med.*, 21, 485, 1997.



92. Funk, J.O., Kruse, A., and Kirchner, H., Cytokine production in cultures of human peripheral blood mononuclear cells, *J. Photochem. Photobiol. B Biol.*, 16, 347, 1992.
93. Naim, J.O., Yu, W. Ippolito, K.M.L., Gowan, M., and Lazafame, R.J., The effect of low level laser irradiation on nitric oxide production by mouse macrophages, *Lasers Surg. Med.*, Suppl. 8, 7 (abstr. 28), 1996.
94. Mrowiec, J., Sieron, A., Plech, A., Cieslar, G., Biniszkiewicz, T., and Brus, R., Analgesic effect of low-power infrared laser radiation in rats, *Proc. SPIE*, 3198, 83, 1997.
95. Vladimirov, Y., Borisenko, G., Boriskina, N., Kazarinov, K., and Osipov, A., NO-hemoglobin may be a light-sensitive source of nitric oxide both in solution and in red blood cells, *J. Photochem. Photobiol. B Biol.*, 59, 115, 2000.
96. Sbarra, A.J. and Strauss, R.R., Eds., *The Respiratory Burst and Its Photobiological Significance*, Plenum Press, New York, 1988.
97. Sharp, R.E. and Chapman, S.K., Mechanisms for regulating electron transfer in multi-centre redox proteins, *Biochem. Biophys. Acta*, 1432, 143, 1999.

